

A Constraint based Statistical Approach to Failure from Complex Defects

Bostjan Bezensek^{*} and John W. Hancock

University of Glasgow, Mechanical Engineering Department, Glasgow, UK

ABSTRACT: *Structural failure from complex defects is examined by including the constraint effects within a statistical weakest link analysis. The method allows the failure probabilities of arbitrary geometries to be compared and identifies the most likely failure initiation site for a complex defect. The analysis can be generalised to problems in which toughness varies with the spatial position of the crack front, as in the case of a crack located in a temperature gradient or subject to embrittlement.*

1. INTRODUCTION

Defects in engineering structures frequently have complex shapes. Assessment procedures re-characterise these defects as simpler shapes, which are more amenable to analysis. This is conservative as long as the re-characterised defect is more detrimental than the original defect. This process was developed for defects extending by fatigue, but is frequently applied to monotonic loading. In the current work the re-characterisation procedure is applied to defects which extend by cleavage [1]. Cleavage failures are inherently statistical, and are frequently discussed using weakest link arguments in which the local fracture toughness is considered to be a statistically distributed material property (Wallin [2], Slatcher *et al* [3]).

The work extends methods developed by Slatcher *et al* [3] for defect assessment problems in which both the resistance and the crack driving force are spatial functions of the crack tip position. Although more general aspects can be incorporated into the argument, the paper focuses on in-plane constraint effects. The loss of crack tip constraint can be quantified [4] by the non-singular term in the Williams expansion [5], which Rice [6] has denoted the T-stress. The constraint enhanced fracture toughness is quantified by an expression suggested by Wallin [7]:

^{*} On leave from University of Maribor, Faculty of Mechanical Engineering, Slovenia

$$\begin{aligned}
K_{(T)} &= 20 + (K_{IC} - 20) \exp\left\{0.0019\left(-\frac{T}{10}\right)\right\}, & \text{for } T < 0 \\
K_{(T)} &= K_{IC}, & \text{for } T \geq 0
\end{aligned} \tag{1}$$

2. WEAKEST LINK STATISTICS FOR SPATIALLY VARYING CRACK PARAMETERS

Geometry and the crack shape determine the distribution of the applied stress intensity factor, $K_{(t)}$, along the crack front. Let the crack front be divided into m incremental segments of length dt . The probability that a small crack front segment (i) of length dt , will fail at a locally applied stress intensity less than or equal to K is $F^{(i)}$. The survival of the crack front requires survival of all segments, giving:

$$F_{(K)} = 1 - (1 - F^{(i)})^m \tag{2}$$

where m is a large number. Reasonable agreement with experimental cleavage data (Landes and Shafer [8]) can be achieved using a two parameter Weibull function, which can be expressed for a straight crack of length, s , under applied stress intensity, K , as:

$$F_{(K)} = 1 - \exp\left\{-\frac{s}{s_o} \left(\frac{K}{K_o}\right)^n\right\} \tag{3}$$

K_o and s_o are curve fitting parameters, and n is the shape factor which Wallin [9] argues to be 4 in J-dominant fields. Without loss of generality K_o can be replaced with a mean value of the local toughness, $\bar{K} = K_o \Gamma(1 + \frac{1}{n})$, where $\Gamma(1 + \frac{1}{n})$ is the Gamma function. This allows Eq. (3) to be rewritten with a modified constant, s'_o :

$$F_{(K)} = 1 - \exp\left\{-\frac{1}{s'_o} \left(\frac{K}{\bar{K}}\right)^n\right\} \tag{4}$$

In present problem the mean fracture toughness \bar{K} is taken to be a function of constraint, as given by Eq. (1). In a complex defect the

constraint, and thus mean local toughness vary with spatial position, t . This allows Eq. (4) to be written more generally as:

$$F_{(K')} = 1 - \exp \left(- \frac{1}{s'_o} \int_s \left(\frac{K_{(t)}}{K_{(T,t)}} \right)^n dt \right) \quad (5)$$

Under any given loading, the probability of failure, and the most likely site of failure initiation can be determined if the crack front is divided into two segments, A and B, as shown schematically in Figure 1. The probability that failure initiates from segment A requires segment A to fail, while the other segment survives. The total probability of failure of the entire crack is given by moving the boundary, from one extremity of the crack to the other. The most likely (modal) failure initiation site can be determined by differentiating the cumulative probability function (CPF) of (5) along the crack front. The most likely site of failure initiation is the location with the greatest value of the probability density function (pdf).

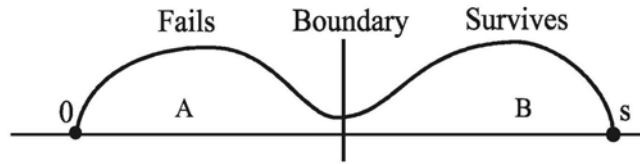


Figure 1: Definition of failure from segment of a complex crack front

This procedure is used to analyse cleavage failures from complex defects, and allows a comparison of the failure probabilities of real and re-characterised defects.

3. EXPERIMENTAL

The experimental work focused on a complex defect, formed by the coalescence of two surface breaking cracks which were developed by fatigue. Experiments were performed on a plain carbon-manganese 50D steel (BS 4360), using three point bend specimens with the geometry shown in Figure 2. Surface breaking defects were produced by fatigue tests on plate

containing two co-planar starter notches, cut with a circular slitting wheel. This procedure resulted in a family of complex defects with pronounced re-entrant sectors, as shown in Figure 3(a) and eventually a bounding semi-elliptical defect, as shown in Figure 3(b). These were tested to failure at -196°C , (representative of the lower shelf) and at -100°C , (representative of the ductile-brittle transition). At -196°C the configurations with pronounced re-entrant sector failed at 75 kN and 85 kN, whereas bounding defect failed at 90 kN and 98 kN [1]. In the tests at -100°C failure loads were 210 kN and 93 kN for re-entrant and bounding geometries.

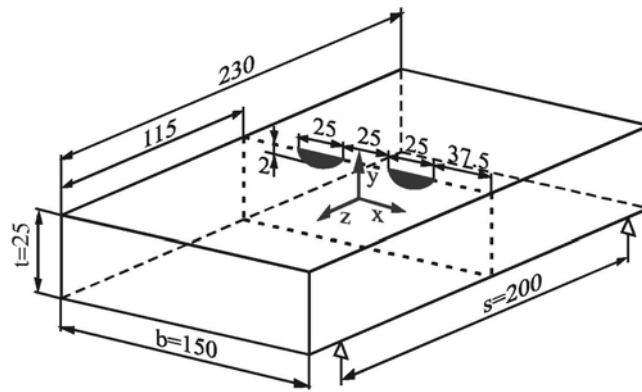


Figure 2: Experimental geometry; all units in [mm]

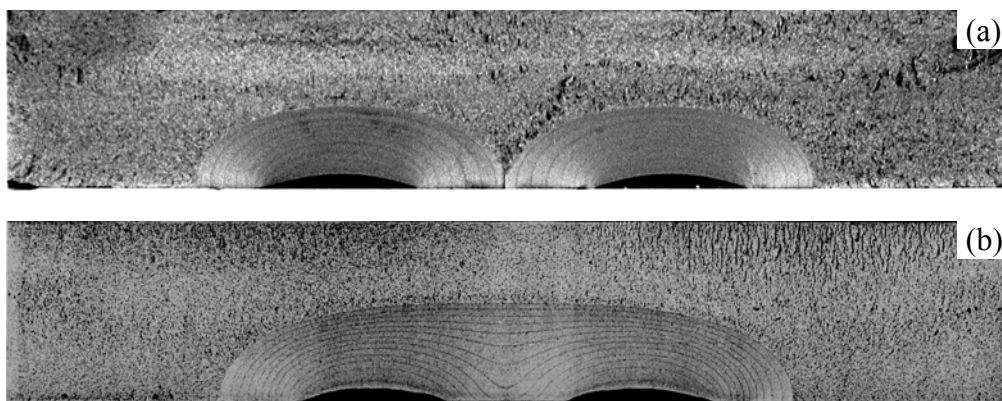


Figure 3: Fracture surface of test specimens with a complex defect and a bounding semi-elliptical defect

4. RESULTS AND DISCUSSION

4.1 Deterministic analysis

The crack profiles were digitised and analysed using the line spring technique of Rice and Levy [10] as implemented in ABAQUS [11] to determine the local stress intensity factor and T-stress. Defects were re-characterised following BS 7910 [12], with a bounding semi-elliptical defect. Results for the re-entrant and re-characterised geometries are presented in Figure 4. Figure 4(a) shows the crack profiles. The normalised stress intensity factors are given in Figure 4(b), and the T-stress normalised with the outer fibre stress is shown in Figure 4(c). Compressive T-stresses and amplified stress intensity factors develop in re-entrant sectors. Limit loads were determined numerically as 208 kN at $-196\text{ }^{\circ}\text{C}$ for the defect with the pronounced re-entrant sector and 225 kN for re-characterised defects and 197 kN and 108 kN for the two defects tested at $-100\text{ }^{\circ}\text{C}$.

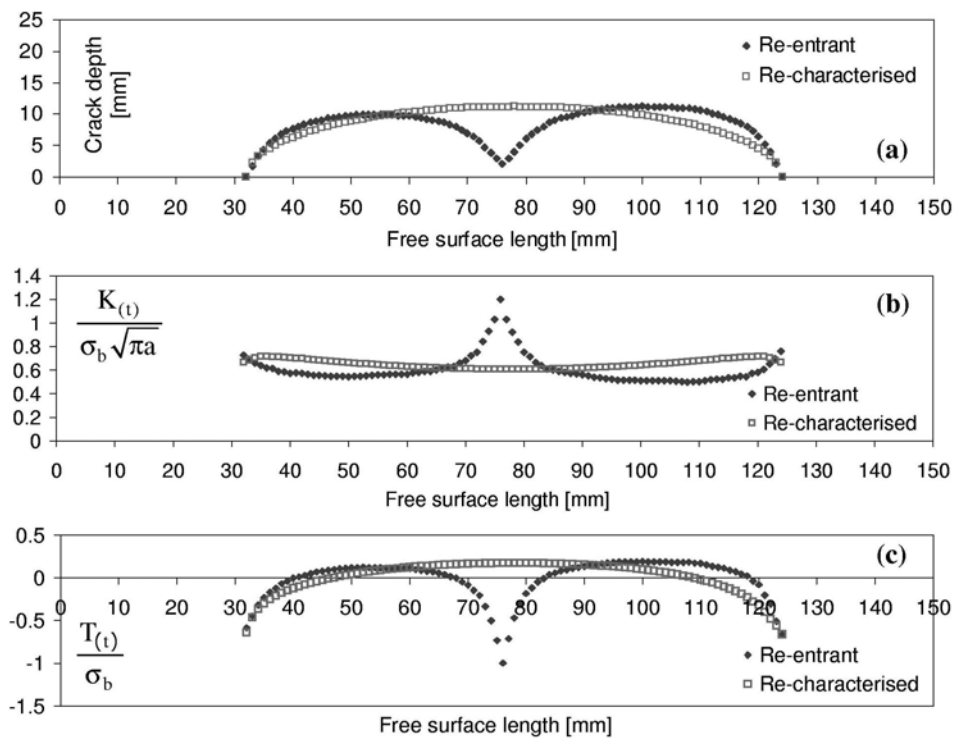


Figure 4: Normalised crack tip parameters obtained from detailed line spring analysis [10] of the test results

- (a) Crack profile of a complex and re-characterised defect
- (b) Normalised stress intensity factors for both defects
- (c) Normalised T-stress for both defects

4.2 Probabilistic analysis

The cumulative probability of failure along the crack front of the complex and re-characterised geometries is given in Figure 5 for the applied failure load of the real defect. For failures at small fractions of the limit load, the constraint effects in pronounced re-entrant sectors are not significant, giving higher failure probability for the real defect with re-entrant sector, as shown in Figure 5(b) over the re-characterised defect. Conversely for failures close to the limit load (-100°C) there is significant constraint loss in the shallow re-entrant sector, decreasing the failure probability of the real defect compared to the re-characterised defect, as shown in Figure 5(c). This is consistent with the failure loads observed in the experiments.

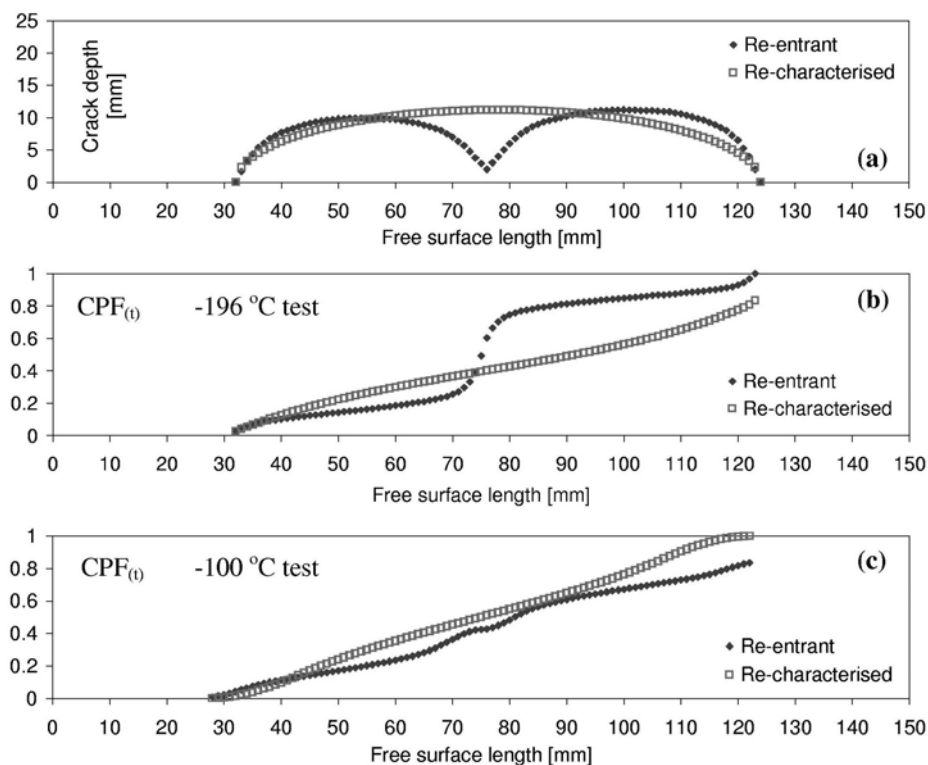


Figure 5: A probabilistic analysis of test results

- (a) Crack profile of a complex and re-characterised defect
- (b) Cumulative probability of failure for both defects at -196°C
- (c) Cumulative probability of failure for both defects at -100°C

4.3 The origin of failure

The most likely site of failure is indicated by the probability density function, shown in Figure 6. The most likely site of failure initiation at small fractions of the limit load is the re-entrant sector, as shown by failure at -196°C , and illustrated in Figure 6(b). For failures close to the limit load the pdf (Figure 6(c)) indicates the most likely failure site are the deeper crack segments close to the re-entrant sector. Although these sites do not have the greatest stress intensity, there are only small constraint enhanced toughness effects.

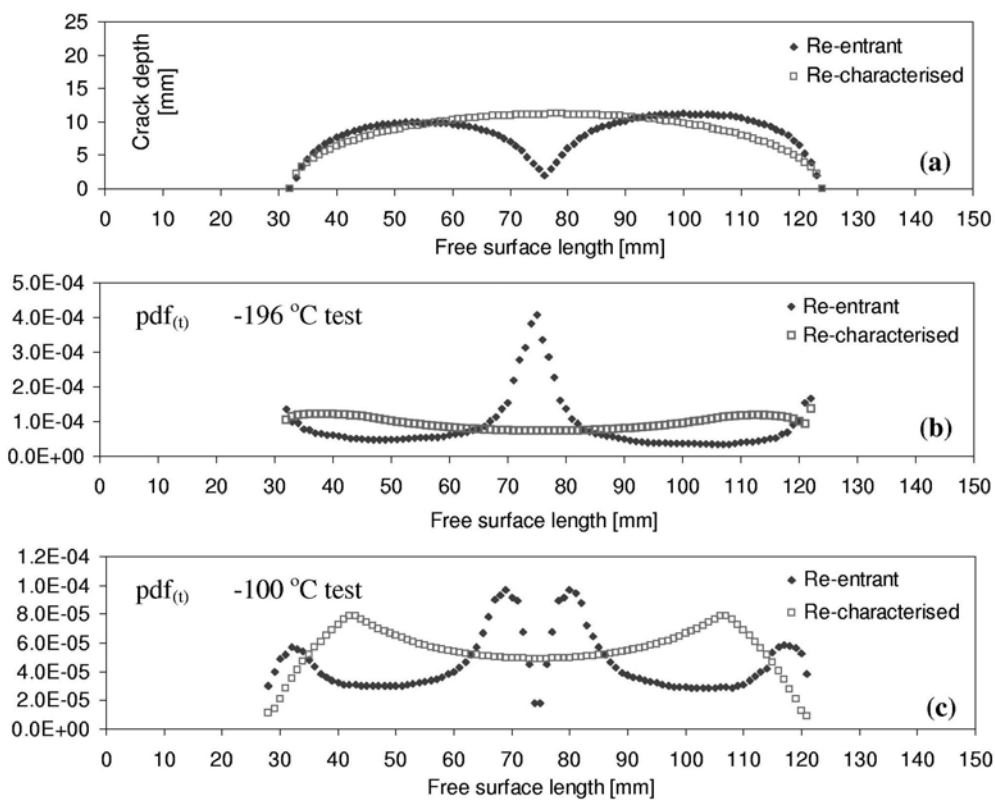


Figure 6: A probabilistic analysis of test results (Part 2)

- (a) Crack profile of a complex and a re-characterised defect
- (b) Probability density function for both defect at -196°C
- (c) Probability density function for both defect at -100°C

5. CONCLUSIONS

The paper presents a statistical method for assessing the probability of failure for complex defects incorporating in-plane constraint effects. The method has been extended to indicate the most likely failure site from complex crack profiles. The defect re-characterisation process is shown to be conservative in ductile-brittle transition, when in-plane constraint effects are invoked. A potential non-conservative assessment occurs when re-characterisation procedures developed for fatigue are applied to cleavage failures from complex defects [1] on the lower shelf.

6. REFERENCES

- 1 Bezensek, B. and Hancock, J.W. (2002), To be published
- 2 Wallin, K., (1985), *Engineering Fracture Mechanics*, **22**, p.149
- 3 Slatcher, S. and Oystein, E., (1986), *Engineering Fracture Mechanics*, **24**, No.4, p. 495
- 4 Betegón, C. and Hancock, J.W., (1991), *Journal of Applied Mechanics*, **58**, p:104
- 5 Williams, M.L., (1957), *ASME Journal of Applied Mechanics*, **24**, p.111
- 6 Rice, J.,R., (1974), *Journal of The Mechanics and Physics of Solids*, **22**, p: 17
- 7 Wallin, K., (2000), Proceedings ASME PVP2000 conference, **412**, USA, July 2000
- 8 Landes, J.D. and Shaffer, D.H., (1980), In “Fracture Mechanics: Twelfth Conference”, ASTM STP 700
- 9 Wallin, K., (1984), *Engineering Fracture Mechanics*, **19**, p.1085
- 10 Rice, J.R. and Levy, N., (1972), *Journal of Applied Mechanics*, **39**, No. 1, March 1972, p: 185
- 11 HKS, (1998), ABAQUS/Standard, v5.8, Hibbitt, Karlsson and Sorensen, inc, Providence, Rhoad Island
- 12 BS 7910, (1999), *Guidance on methods for assessing the acceptability of flaws in metallic structures*, British Standard Institution, London, UK